Turkish Journal of Computer and Mathematics Education Vol.12 No.13(2021), 2453-2464

Research Article

MHD Mixed Convection Jeffrey Fluid Near a Stagnation-Point Flow of Induced Magnetic Field and Linear/Non-Linear Vertical Stretching Sheet with Chemical Reaction in The Presence of Thermal Radiation and Suction or Injection

G.Kathyayani[1*], R. Lakshmi Devi[1]

[1*] Department of Applied Mathematics, YogiVemana University,Kadapa,Andhra Pradesh-516005,India

[1] Department of BS & H (Mathematics), Siddharth Institute of Engineering & Technology (Autonomous), Puttur, Andhra Pradesh-517583, India

Article History: Received: 11 January 2021; Revised: 12 February 2021; Accepted: 27 March 2021; Published online: 4 June 2021

Abstract: The effect of induced magnetic field and chemical reaction with linear / non-linear vertical stretching sheet of mixed convection Jeffrey fluid near a stagnation point flow through porous medium in the presence of thermal radiation and slip flow regime is analyzed. The set of coupled governing non-linear partial differential equations are transformed into a set of coupled non-linear ordinary differential equations using suitable similarity transformations, which are then solved numerically using Runge-Kutta fourth order in association with shooting technique in MATLAB. The effects of non-dimensional parameters such as Jeffrey parameter, Magnetic force number, magnetic Prandtl number, magnetic parameter, suction/injection parameter, slip velocity parameter, linear or non-linearity parameter, permeability parameter, velocity ratio parameter, Prandtl number, thermal radiation parameter, chemical reaction parameter, Grashof number and Eckert number on velocity, temperature induced magnetic field and concentration are presented graphically while the skin friction, local Nusselt number and Sherwood number are represented numerically with tables.

Key words: Chemical reaction, Induced Magnetic number, Jeffrey parameter, MHD mixed, convection, non-linearly stretching sheet, Porous medium, slip flow, thermal, radiation, viscous dissipation.

1. Introduction

The flow of stagnation point was initially studied by Pai [14]. Later, the flow over a stretching sheet and obtaining similarity solution in closed analytical form was investigated by Crane [5]. Now- a- days the study of stagnation flow near a stretching sheet is essential in manufacturing processes and industries. For example, the study of the biological fluids in the occurrence of magnetic fields(biomagnetic fluid flow)near a stretching sheet is much essential applications in medical field and bioengineering area. Interest in magnetohydrodynamic flow began in 1918, when Hartmann (see Rossow [17]) invented the electromagnetic pump. Further, the study of MHD stagnation point flow of an electrically conducting fluid has numerous applications. Some of which are originated in the sphere of chemical engineering and metallurgy process such as drawing, strengthening and thinning of copper wire, etc. The induced magnetic field has established much interest due to its practice in many scientific and technological phenomena, for example, in MHD energy generator systems and magnetohydrodynamic boundary layer control technologies. Denno and Fouad [6] investigated the effects of a non-uniform magnetic field on MHD channel flow between two parallel plates of infinite extent. Influence of the induced magnetic field such that the magnetic Reynolds number is less than unity but greater than zero is included. The goal is to use the MHD effect to reduce the amount of heat transfer from the fluid to the channel walls.

The non-Newtonian fluids are found in many engineering and industrial processes such as blood, food mixing and chime movement in the intestine, flow of blood, flow of plasma, flow of mercury amalgams and lubrications with heavy oils and greases. Such fluids don't obey the Newton's law of viscosity and are usually called non- Newtonian fluids. The study of non-Newtonian fluids has much interest because of their numerous technological applications, movement of biological fluids and performance of lubricants including manufacturing of plastic sheets, thermal oil

recovery and transpiration cooling. In view of their differences with Newtonian fluids, several models of non-Newtonian fluids are projected by various researchers. Among these, the Jeffrey model is a rate type of non-Newtonian fluid which can describe the characteristics of relaxation and retardation times.

Ghosh et al., [7] analytically studied the impacts of magnetic induction and transverse magnetic field on natural convection MHD boundary layer flow over an infinite vertical flat plate. Ali et al., [1] studied the steady magnetohydrodynamic boundary layer flow and heat transfer of a viscous and electrically conducting fluid over a stretching sheet and further investigated on steady MHD stagnation-point flow of an incompressible viscous fluid over a stretching sheet and the effect of an induced magnetic field is taken into account. Unsteady MHD flow near a stagnation point of a two-dimensional porous body with heat and mass transfer in the presence of chemical reaction and thermal radiation has been numerically investigated Stanford Shateyi and Marewo [21]. Jayachandra Babu et al., [9] analyzed the effects of non-linear thermal radiation and induced magnetic field on nano ferrofluid particle flows near a stagnation-point flow towards a stretching sheet in the presence of non-uniform heat source/sink.

Raju et al., [15] and Shit and Roy [20] analyzed "The effect of induced magnetic field" on non-Newtonian fluid near a stagnation-point flow over a stretching sheet with homogeneous–heterogeneous reactions" and non-uniform heat source or sink and they considered the effect of the induced magnetic field is taken into account. Sandeep et al., [18] investigated the MHD stagnation point Jeffrey nanofluid flow of heat and mass transfer behaviour over a stretching surface in the presence of chemical reaction and induced magnetic field and non-uniform heat source or sink. The study of MHD stagnation point flow of Casson liquid towards a stretched surface in the presence of chemical reaction model involving both heat and mass transfer is established Ijaz Khan et al., [8]. Animasaun et al., [2] has done analysis on MHD mixed convection buoyancy-driven stagnation-point flow of dust nanofluid particles embedded over an inclined non-isothermal stretching sheet in the presence of induced magnetic field and non-uniform heat source/sink and suction. Two types of nanofluids namely Cu-water and Al_2O_3-water embedded with conducting dust particles is considered.

Recently Nandkeolyar et al., [13] studied two-dimensional laminar viscous, incompressible boundary layer flow of mixed convective and electrically conducting fluid under the influence of an aligned magnetic field which is applied along the flow outside the boundary layer. Athira et al., [4] observed the impacts of induced magnetic field and non-linear convection in the flow of viscous fluid over a porous plate under the influence of chemical reaction and heat source/sink. Mohamed Abd El-Aziz and Ahmed [11]investigated the effect of induced magnetic field on MHD Casson fluid near a stagnation-point flow and heat transfer over a stretching surface. The bio-magnetic fluid (BMF) flow and heat transfer in the three-dimensional unsteady stretching/shrinking sheet is examined Murtaza et al., [12]. They studied that the version of bio-magnetic fluid dynamics (BFD) which is consistent with the principles of ferrohydrodynamics (FHD)be used in bio-medical and bio-engineering applications. Mohamed Abd El-Aziz and Afify [11] have numerically investigated the steady MHD boundary layer flow near a stagnation point over a stretching surface in the presence of the induced magnetic field, viscous dissipation, magnetic dissipation, slip velocity phenomenon and heat generation/ absorption effects.

In the present paper, we have investigated the effect of induced magnetic field and chemical reaction on MHD mixed convection Jeffrey fluid near a stagnation-point flow of induced magnetic field and linear/non-linear vertical stretching sheet with chemical reaction in the presence of thermal radiation and suction or injection. The set of coupled governing non-linear partial differential equations are transformed into a set of coupled non-linear ordinary differential equations using some suitable similarity transformations and then solved numerically using Runge-Kutta fourth order in addition with shooting technique in MATLAB. The motivation behind this study is to consider the effect of induced magnetic field and chemical reaction on mixed slip flow of MHD nearby a stagnation-point on a non-linearly vertical stretching sheet in the existence of viscous dissipation and thermal radiation Shateyi and Mabood [19].The effects of linear or non-linear parameter m ($m=1$ or $m=2$), suction/injection parameter f_w, mixed convection parameter λ , induced magnetic constant M_1 , magnetic force number M_f ,magnetic Prandtl number Pm and other above mentioned parameters on velocity $f'(\eta)$, temperature $\theta(\eta)$, induced magnetic field $H(\eta)$ and

concentration profile $\varphi(\eta)$ are represented graphically while the Sherwood number, skin friction and local Nusselt number are presented numerically with tables.

2. Mathematical Formulation of The Problem

The steady two-dimensional conducting mixed convection Jeffrey fluid near a stagnation point flow of vertical plate embedded in a porous medium with the effect of induced magnetic field and linear or non-linearly stretching sheet and suction or injection in the presence of chemical reaction and slip flow regime is considered. Here the prescribed surface heat flux is also considered. The *x*-axis is considered as stretching sheet and *y*-axis is normal to it and the flow is confined in half plane y>0. A uniform magnetic field of strength *B*(*x*) is applied in the direction of normal to the surface as shown in Figure 1. The stretching sheet velocity is supposed to be $u_w(x) = c\,x^m$ and $u_e(x) = a\,x^m$ as an external velocity, where *c* and *a* are positive constants. While *m* is the linearity parameter with $m = 1$ for the linear case and $m \neq 1$ for the non-linear case. The fluid velocity vector and induced magnetic field vector are assumed as $\vec{q} \equiv (u, v, 0)$, $\vec{H} \equiv (h_x, h_y, 0)$ where u, v, h_x and h_y are the components of fluid velocity and induced magnetic field.

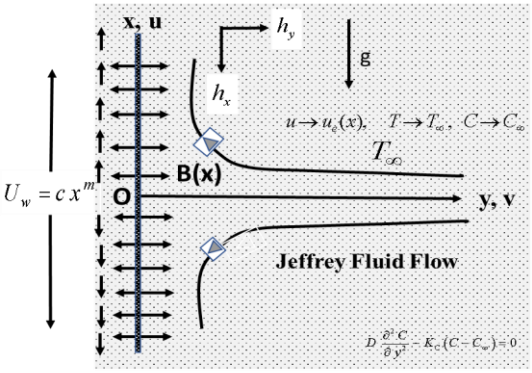

Figure 1. Physical model

Under the above assumptions and the boundary-layer and Boussinesq approximation, the governing equations for the current study are given by(Shateyi and Mabood [19]):

$$\frac{\partial u}{\partial x} + \frac{\partial v}{\partial y} = 0 \tag{1}$$

$$\frac{\partial h_x}{\partial x} + \frac{\partial h_y}{\partial y} = 0 \tag{2}$$

$$u\frac{\partial u}{\partial x} + v\frac{\partial u}{\partial y} = u_e\frac{d u_e}{d y} + \frac{\upsilon}{1+\lambda_1}\frac{\partial^2 u}{\partial y^2} - \frac{\sigma B^2(x)}{\rho}(u_e - u) - \frac{\upsilon}{k}u + g\beta(T - T_\infty) + g\beta_C(C - C_\infty) + \frac{u_e H_0}{\rho}\frac{\partial h_x}{\partial y} \tag{3}$$

$$u\frac{\partial h_x}{\partial x} + v\frac{\partial h_x}{\partial y} = h_x\frac{\partial u}{\partial x} + h_x\frac{\partial u}{\partial y} + \alpha_m\frac{\partial^2 h_x}{\partial y^2} \tag{4}$$

$$u\frac{\partial T}{\partial x} + v\frac{\partial T}{\partial y} = \alpha\frac{\partial^2 T}{\partial y^2} - \frac{1}{\rho\ Cp}\frac{\partial q_r}{\partial y} + \frac{\mu}{\rho Cp}\left(\frac{\partial u}{\partial y}\right)^2 \tag{5}$$

$$u\frac{\partial C}{\partial x} + v\frac{\partial C}{\partial y} = D\frac{\partial^2 C}{\partial y^2} - K_C(C - C_\infty) \tag{6}$$

The corresponding boundary conditions to the current model is given by:

$$u = u_w(x) + \frac{2-\delta_v}{\delta_v}\lambda_0\frac{\partial u}{\partial x}, \quad v = v_w(x), \quad \frac{\partial H}{\partial y} = -\frac{H_w(x)}{H_0}, \quad \frac{\partial T}{\partial y} = -\frac{q_w(x)}{k}, \quad \frac{\partial C}{\partial y} = -\frac{C_w(x)}{K_C} \quad \text{at} \quad y = 0 \tag{7}$$

$$u \to u_e(x), \qquad T \to T_\infty \qquad h_x \to 0, \qquad C \to C_\infty \qquad \text{as} \quad y \to \infty \tag{8}$$

By using the Rosseland diffusion approximation, Anwar Hossain *et al.*, [3], Raptis [16] among other researchers the radiative heat flux q_r is given by:

$$q_r = -\frac{4\sigma^* T_\infty^3}{3K_s}\frac{\partial T^4}{\partial y} \tag{9}$$

We assume that the temperature differences within the flow are sufficiently small, so that T^4 may be expressed as a linear function of temperature T.

$$T^4 \approx 4T_\infty^3 T - 3T_\infty^3 \tag{10}$$

Using eqs. (9) and (10) in the fourth term of eq. (5) we obtain:

$$\frac{\partial q_r}{\partial y} = -\frac{16\sigma^* T_\infty^3}{3K_s}\frac{\partial^2 T}{\partial y^2} \tag{11}$$

3. Similarity analysis

we define the following similarity transformations as followed by Shen et al., [10]:

$$\eta = \sqrt{\frac{a}{\nu}}\, y\, x^{\frac{m-1}{2}}, \quad \psi = \sqrt{a\nu}\; x^{\frac{m+1}{2}} f(\eta), \quad \theta = \sqrt{\frac{a}{\nu}}\,\frac{k(T-T_\infty)}{q_0\; x^{2m-1}}, \quad H = \frac{x^{\frac{3m-1}{2}} H_0}{\sqrt{\frac{a}{\nu}}} h_x \quad \phi = \sqrt{\frac{a}{\nu}}\,\frac{K_C(C-C_\infty)}{C_0\; x^{2m-1}} \tag{12}$$

Here ψ is the stream function such that $u = \frac{\partial \psi}{\partial y},\ v = -\frac{\partial \psi}{\partial x}$ and continuity equation is automatically satisfied. By using eq. (12), the velocity components for u and v are given:

$$u = a\, x^m\; f'(\eta), \qquad v = -\sqrt{a\nu}\, x^{\frac{m-1}{2}}\left[\frac{m+1}{2} f(\eta) + \frac{m-1}{2}\eta\; f'(\eta)\right] \tag{13}$$

where primes denote differentiation with respect to η. We remark that to obtain similarity solutions, $B(x)$, $v_w(x)$ and $q_w(x)$ are taken:

$$B(x) = B_0\, x^{\frac{m-1}{2}}, \quad v_w = -\frac{\sqrt{a\nu}(m+1)}{2}\, x^{\frac{m-1}{2}}\; f_w, \quad H_w(x) = H_0\; x^{2m-1}, \quad q_w(x) = q_0\; x^{\frac{5m-1}{2}} \quad C_w(x) = C_0\; x^{\frac{5m-1}{2}} \tag{14}$$

where $B_0, f_w, \mathrm{H}_0, C_0$ and q_0 are arbitrary constants. We also have $f_w > 0$ and $f_w < 0$ are the injection and suction cases respectively and substituting the similarity variables in equationss. (3-6) we obtain the following system of ODE:

$$\frac{1}{(1+\lambda_1)} f''' + \left(\frac{m+1}{2}\right) f\; f'' - m\left(1 - f'^2\right) - \left(\frac{1}{K} + M\right)(1 - f') + \lambda\theta + Gm\;\phi + M_1\frac{\partial H}{\partial \eta} = 0 \tag{15}$$

$$H'' + M_f\left\{\left(\frac{m+1}{2}\right) f\, H' - (2m-1) f' H + Pm\, f''\right\} = 0 \tag{16}$$

$$\left(1 + \frac{4}{3R}\right)\theta'' + \mathrm{Pr}\left\{\left(\frac{m+1}{2}\right) f\,\theta' - (2m-1) f'\theta + Ec\left(f''\right)^2\right\} = 0 \tag{17}$$

$$\phi'' + Sc\left\{\left(\frac{m+1}{2}\right) f\,\phi' - (2m-1) f'\phi - \gamma\;\phi\right\} = 0 \tag{18}$$

the corresponding boundary conditions `are:

$$f(0) = f_w, \qquad f'(0) = \varepsilon + \delta f''(0), \qquad H'(0) = -1, \qquad \theta'(0) = -1, \quad \phi'(0) = -1 \tag{19}$$

$$f'(\infty) = 1, \qquad H(\infty) = 0, \qquad \theta(\infty) = 0, \qquad \phi(\infty) = 0 \tag{20}$$

Where $M = B_0^2/\rho a$, $\lambda = g\beta q_0 (v)^{1/2}/k\, a$, $M_1 = \nu H_0\; x^{2m}/a^2\,\rho$, $M_f = a^2\,\nu H_0\; x^{m-3}/\alpha_m$, $\mathrm{Pm} = \nu H_0/\rho\sqrt{a}$, $\varepsilon = {}^{C}/_{a}$

$\mathrm{Pr} = \nu/\alpha$, $Ec = a^{5/2} x^{3m}/\rho Cp$, $R = 4\sigma^* T^3/\rho Cp\, k_1$, $\delta = (2-\sigma_v) k\, x_n\, \mathrm{Re}_x^{1/2}/\sigma_v$, $Gm = \frac{\nu g\,\beta_c (C - C_\infty)}{x^{2m-1}}$, $Sc = \frac{\nu}{D}$,

$\gamma = \frac{Kc\;\nu}{x^{2m-1}}$, $K = \frac{k\, a\, x^{m-1}}{\nu}$

4. Local Skin Friction, Nusselt Number and Sherwood Number

The physical parameters interest for the present problem are the local skin friction coefficient C_f , the local Nusselt number Nu_x and local Sherwood number Sh_x which are defined as:

$$C_f = \frac{\tau_w(x)}{\rho(1+\lambda_1)u_p^2}, \quad Nu_x = \frac{x q_w(x)}{k(T_w - T_\infty)}, \qquad Sh_x = \frac{x c_w(x)}{\mathrm{K_C}(\mathrm{C}-C_\infty)} \tag{21}$$

with the surface shear stress $\tau_w(x) = \partial u/\partial y]_{y=0}$ and $q_w(x)$ is the wall heat flux. We then obtain the following expressions after applying the similarity variables:

$$\mathrm{Re}_x^{1/2}\ C_f = \frac{f''(0)}{(1+\lambda_1)}, \qquad \mathrm{Re}_x^{1/2}\ Nu_x = \frac{1}{\theta'(0)}, \qquad \mathrm{Re}_x^{1/2}\ Sh_x = \phi'(0) \tag{22}$$

with $\mathrm{Re}_x = u_e\, x/\nu$ being the Reynolds number. Numerical values of the function $f''(0)$, $\theta'(0)$ and $\phi'(0)$ which represent the wall shear stress, the heat transfer rate and local Sherwood number at the surface respectively for various values of the parameter are presented in Table 1.

5. Results and discussion

In this article we analyze the effect of induced magnetic field and chemical reaction on mixed convection Jeffrey fluid near a stagnation point flow with a linear / non-linear vertical stretching sheet through porous medium in the presence of slip flow regime. The boundary value problem containing coupled equations in velocity, temperature, induced magnetic field and concentration are solved numerically by shooting technique with Runge-Kutta fourth order using MATLAB.

The effects of linear or non-linear parameter m ($m=1$ or $m=2$), suction/injection parameter f_w, mixed convection parameter λ , induced magnetic constant M_1, magnetic force number M_f ,magnetic Prandtl number Pm , Jeffrey parameter λ_1 , chemical reaction parameter γ ,Schmidtnumber Sc ,Grashof number Gm , Magnetic parameter M , porous medium parameter K , the velocity slip parameter δ , velocity ratio parameter ε , Prandtl number Pr ,Eckert number Ec and thermal Radiation parameter R are depicted through graphs on velocity $f'(\eta)$, temperature $\theta(\eta)$, induced magnetic field $H(\eta)$ and concentration $\phi(\eta)$ profiles with fixed values of $\lambda_1 = 2$, $M_f = 0.5$ $Pm = 0.5$, $M_1 = 0.5$, $M = 0.5$, $K = 1$, $\delta = 1$, $\varepsilon = 0.5$, $\mathrm{Pr} = 0.7$, $Ec = 1$, $f_w = 1$, $\lambda = 1$, $Sc = 1$, $\gamma = 1$, $Gm = 2$ and $m = 1$ or $m = 2$. In order to assure the accuracy of the applied numerical scheme the computed values of Skin friction coefficient $\frac{f''(0)}{1+\lambda_1}$ and local Nusselt number $-\theta'(0)$ are compared with the available results of Shateyi and Mabood [19] and Wang [22] in Table 1and have found in excellent agreement.

Graphical representations of the numerical results are illustrated in figs.2-21. From figures2, 3, 4, 5 and 6, illustrates that the effects of magnetic force number M_f , Jeffrey parameter λ_1 , the velocity slip parameter δ , Grashof number Gm and porous medium parameter K , on the velocity distribution for both assisting $(\lambda = 1)$ and opposing $(\lambda = -1)$ cases vary with linear $(m = 1)$ and non-linear $(m = 2)$ in the presence of with and without($M_1 = 0$ and $Gm = 0$) induced magnetic field and concentration. It is observed that velocity exponentially growths with an increasing of magnetic force number M_f ,Jeffrey parameter λ_1 ,slip parameter δ ,Grashof number Gm and porous medium parameter K , for all the cases of linear $(m = 1)$, non-linear $(m = 2)$ vary with assisting flow $(\lambda = 1)$, but the opposite behavior is observed for opposing flow $(\lambda = -1)$ .This is due to the fact that the presence of the non-Newtonian characteristics of Jeffrey fluid flows which decrease the velocity and the boundary layer thickness as well.

And it is observed that the velocity attains the maximum value at $M_1 = Pm = 0$, ie. without induced magnetic field and concentration. The opposite behavior is observed for the induced magnetic constant M_1 and magnetic number M from figures 7 and 8. This is due to the fact that the presence of transverse magnetic field sets in Lorentz force, which results in retarding force on the velocity field. Therefore, as the values of M increase, so does the retarding force and hence the velocity decreases. The velocity attains the maximum value at $M_1 = Pm = 0$, ie. without induced magnetic field and concentration.

Figures 9 and 10demonstrates the influence of velocity ratio parameter ε and mixed buoyancy parameter λ, on the velocity distribution for both assisting $(\lambda = 1)$ and opposing $(\lambda = -1)$ cases in addition with linear $(m = 1)$ and non-linear $(m = 2)$ in the presence of with and without($M_1 = Pm = 0$) induced magnetic field and concentration. It can be seen that increase of ε and λ causes the velocity profiles to increase.

Figure 11 reveals the influence of suction/injection parameter f_w on the velocity distribution for both assisting and opposing cases vary with linear $(m = 1)$ and non-linear $m = 2$ in the presence of with and without($M_1 = Pm = 0$) induced magnetic field and concentration. It can be seen that the velocity profiles are significantly influenced by suction/injection parameter f_w. The velocity decreases with an increasing of suction parameter $f_w = -1,\ 0,\ 1$.

Figures 12 and 13 represent the effects of Prandtl number $\Pr$, thermal radiation parameter R on the temperature distribution for both assisting $(\lambda = 1)$ and opposing $(\lambda = -1)$ cases vary with linear $(m = 1)$ and non-linear $m = 2$ in the presence of with and without($M_1 = Pm = 0$)induced magnetic field. It can be observed that the temperature profiles are significantly influenced by $\Pr$ and R. The temperature decreases with an increasing of $\Pr$ and R with linear $m = 1$ and non-linearity value $m = 2$. This is due to the fact that a higher Prandtl number fluid has relatively low thermal conductivity, which reduces conduction and there by the thermal boundary layer thickness and as a result, temperature decreases. The opposite behavior is observed for the Eckert number Ec, from figure 14. The temperature profile attains the minimum value for all the cases at $M_1 = Pm = 0$, ie. without induced magnetic field and concentration.

The effect of Jeffrey fluid parameter λ_1,on the temperature distribution is observed from the figure 15, for both assisting $(\lambda = 1)$ and opposing $(\lambda = -1)$ cases vary with linear $(m = 1)$ and non-linear $m = 2$ in the presence of with and without ($M_1 = Pm = 0$)induced magnetic field and concentration. It can be seen that increasing the Jeffrey fluid parameter λ_1, causes the temperature profiles to increase for the case of $m = 2, \lambda = 1$ and $m = 1, \lambda = 1$, but the opposite trend is observed for the case of $m = 2, \lambda = -1$.

Figures16 and 17, depicts the influence of the induced magnetic constant M_1 and magnetic Prandtl number Pm on induced magnetic field for both assisting $(\lambda = 1)$ and opposing $(\lambda = -1)$ cases vary with linear $m = 1$ and non-linear $m = 2$. It can be observed that the induced magnetic field profiles are significantly influenced by M_1 and Pm. The induced magnetic field increases with an increasing of M_1 and Pm. It is also observed that the induced magnetic field profile attains the maximum value for the values of $m = 1$ and $(\lambda = 1)$. The opposite behavior is observed for the magnetic force number M_f, from the figure 18.

The influence of Schmidt number Sc, the chemical reaction parameter γ and Grashof number Gm on concentration profile is illustrated in figures19, 20 and 21,for both assisting $(\lambda = 1)$ and opposing $(\lambda = -1)$ cases vary with linear $m = 1$ and non-linear $m = 2$. The concentration profile decreases with an increasing of Sc, γ and Gm.

6. Conclusions

Numerically investigate the effect of induced magnetic field and concentration on mixed convection Jeffrey fluid near a stagnation point flow of a linear / non-linear vertical stretching sheet through porous medium in the presence of slip flow regime. The boundary value problem containing coupled equations in velocity, temperature, induced magnetic field and concentration are solved numerically by shooting technique with Runge-Kutta fourth order using MATLAB. Further numerical results for the skin friction coefficient, Nusselt number and Sherwood number at the surface are in good agreement with the results which were obtained by earlier researchers in the absence of Jeffrey parameter λ_1, Porous medium parameter K, induced magnetic constant M_1 and Grashof number Gm.

- The governing coupled equations are solved numerically by shooting technique with Runge-Kutta fourth order with MATLAB.
- We conclude that

  (i) The velocity decreases with increase of M_1, M and f_w.

  (ii)The temperature decreases with increasing of $\Pr$, R and λ_1.

  (iii)The induced magnetic field decrease with an increasing of M_f and Pm.

  (iv) The concentration profile decreases with an increasing of Sc, γ and Gm.

  And also the velocity increases with increase of M_f, λ_1, δ, Gm, K, ε and λ as well as the temperature increases with increasing of Ec for different aspects ($\lambda = 1, \lambda = -1$ with $m = 1, 2$) and also the induced magnetic field increases with an increasing of induced magnetic constant M_1

- Table 1 shows that the skin friction coefficient $f''(0)$ increases with the increasing values of the Jeffrey fluid parameter λ_1 and porous medium K and also decreasing with the vales of chemical reaction parameter γ and induced magnetic constant M_1. Further it is observed that the values of the Nusselt number $-1/\theta'(0)$ at the surface. From this table it is detected that the rate of heat transfer $-1/\theta'(0)$ decreases with increasing of Jeffrey fluid parameter λ_1 and porous medium K. As well as from it is observed that the values of Sherwood number $\phi'(0)$ increases with an increasing of λ_1, K, γ.

Table 1: Assessment of $-f''(0)$, $-1/\theta'(0)$ and $\phi'(0)$ for various values of λ_1, K, γ and M_1 for fixed values of $\lambda_1 = 2$, $M_f = 0.5$ $Pm = 0.5$, $M_1 = 0.5$, $M = 0.5$, $K = 1$, $\delta = 1$, $\varepsilon = 0.5$, $\Pr = 0.7$, $Ec = 1$, $f_w = 1$, $\lambda = 1$, $Sc = 1$, $\gamma = 1$, $Gm = 2$ and $m = 1$ or $m = 2$.

λ_1	γ	K	M_1	**Present study** $M = 2, \varepsilon = 0.5, \Pr = 0.7$ $f_w = Ec = \delta = 1$			**Shateyi and Mabood**[19] $\delta = \epsilon = \lambda = M = Pr = f_w = 1$, $\lambda_1 = 0$ $K = 0$, $\gamma = 0$, $M_1 = 0.5$		**Wang [22]** $\delta = \epsilon = \lambda = M = M_1 = Pr = \gamma = f_w = 0$ $\lambda_1 = 0$, $m = 1$	
				$f''(0)$	$\theta'(0)$	$\phi'(0)$	$f''(0)$	$\theta'(0)$	for ϵ	$f''(0)$
1	2	1	0.5	0.2517	1.8926	1.0245	0.1547	1.1196	0	1.2342
2	2	1	0.5	0.4875	1.8872	1.1257	0.2123	1.0690	0.1	1.1454
3	2	1	0.5	0.6875	1.7552	1.2672	0.2358	0.9685	0.2	1.0122
1	2	1	0.5	0.6579	1.8952	1.2245	0.1152	1.1176	0.3	0.9873
1	2	2	0.5	0.7187	1.7586	1.2684	0.1587	0.8712	0.4	0.8326

1	2	3	0.5	0.8723	1.6324	1.3625	0.1926	0.7215	0.5	0.7252
1	2	1	0.5	0.7586	1.8926	1.1259	0.1547	1.1196	0.5	0.6524
1	4	1	0.5	0.6875	1.8926	1.3234	0.1547	1.1196	0.5	0.6524
1	6	1	0.5	0.6125	1.8926	1.5246	0.1547	1.1196	0.5	0.6524
1	2	1	0.5	0.2517	1.8926	1.0245	0.1547	1.1196	0.5	0.6524
1	2	1	1	0.1526	1.8926	1.0245	0.1547	1.1196	0.5	0.6524
1	2	1	1.5	0.0918	1.8926	1.0245	0.1547	1.1196	0.5	0.6524

- After substituting the parameter values as $\lambda_1 = 0$, $M_1 = 0$, $\gamma = 0$, $K = 0$, $\delta = \epsilon = \lambda = M = Pr = f_w = 1$, in the present results for Skin friction, Nusselt number and Sherwood number will be coincide with the results of Stanford Shateyi and Mabood [19]. In addition to the after substituting the parameter values $\delta = \epsilon = \lambda = M = Pr = f_w = 0$ and $m = 1$ in the present work we obtain good agreement is originated with the existing results of Wang [22].

Figure. 2: Velocity profile for different values of magnetic force number M_f

Fig. 3: Velocity profile for different values of Jeffrey fluid parameter λ_1

Fig. 4: Velocity profile for different values of the slip velocity parameter δ

Fig. 5: Velocity profile for different values of Grashof number Gm

Fig. 6: Velocity profile for different values of porous medium parameter K

Fig. 7: Velocity profile for different values of induced magnetic constant M_1

Fig. 8: Velocity profile for different values of magnetic parameter M

Fig. 9: Velocity profile for different values of velocity ratio parameter ε

Fig. 10: Velocity profile for different values of mixed convection parameter λ

Fig. 11: Velocity profile for different values of suction/injection parameter f_w

Fig. 12: Temperature profile for different values of Prandtl number $\Pr$

Fig. 13: Temperature profile for different values of Thermal Radiation parameter R

Fig. 14: Temperature profile for different values of Eckert number Ec .

Fig. 15: Temperature profile for different values of Jeffrey fluid parameter λ_1

Fig. 16: Induced magnetic field profile for different values of induced magnetic constant M_1

Fig. 17: Induced magnetic field profile for different values of magnetic force number M_f

Fig. 18: Induced magnetic field profile for different values of magnetic Prandtl number Pm

Fig. 19: Concentration profile for different values of Schmidt number Sc

Fig. 20: Concentration profile for different values of chemical reaction parameter γ

Fig. 21: Concentration profile for different values of Grashof number Gm

7. References

1. Ali F. M, Nazar. R, Arifin. N. M and Prop I; MHD stagnation-point flow and heat transfer towards stretching sheet with induced magnetic field, Appl. Math. Mech. – Engl. ED, 2011,32(4),409-418.DOI 10.1007/s10483-011-1426-6.
2. Animasaun. I. L, Prakash. J, Vijayaragavan. R and Sandeep. N;Stagnation flow of nanofluid embedded with dust particles over an inclined stretching sheet with induced magnetic field and suction, Journal of Nanofluids, 2017, 6(1), 1–10. doi:10.1166/jon.2017.1308.
3. Anwar Hossain. M, Khalil Khanaferand Kambiz Vafai; The effect of radiation on free convection flow of fluid with variable viscosity from a vertical porous plate, Int. J. Therm. Sci, 2001,40(2), pp. 115-124.
4. Athira.P.R, Mahanthesh.B, Gireesha. B.J and Makinde. O.D; Non-linear convection in chemically reacting fluid with an induced magnetic field across a vertical porous plate in the presence of heat source/sink.Defect and Diffusion Forum, 2018, 387, 428-441.doi: 10.4028/www.scientific.net/
5. Crane. L.J; Flow past a stretching plate. ZAMP, 1970, 21, 645-647.
6. Denno. K. I and Fouad. A. A; Effects of the induced magnetic field on the magnetohydrodynamic channel flow, *IEEE transactions on electron devices*, 1972, 39(3), 322-330.
7. Ghosh, S. K, B´eg. O.A and Zueco.J; "Hydromagnetic free convection flow with induced magnetic field effects," Meccanica, 2010, 45(2), 175–185.

8. Ijaz Khan.M, Waqas.M, Hayat.T and Alsaedi.A; Magnetohydrodynamic stagnation point flow of Casson fluid over a stretched surface with homogeneous–heterogeneous reactions, Journal of Theoretical and Computational Chemistry,2017, 16(03).doi.org/10.1142/S0219633617500225**.**
9. Jayachandra Babu. M, Sandeep. N, Raju. C. S. K, Ramana Reddy J. V and Sugunamma. V; Non-linear thermal radiation and induced magnetic field effects on stagnation-point flow of Ferrofluids, Journal of Advanced Physics, 2015, 5, 1–7. doi:10.1166/jap.2015.1271.
10. Ming Shen Ming, Fei Wang and Hui Chen; MHD mixed convection slip flow near a stagnation-pint on a non-linearly vertical stretching sheet, Boundary Value Prob,2015,78,1-15. DOI : 10.1186/s13661-015-0340-6
11. Mohamed Abd El-Aziz and Ahmed Afify. A; Influences of slip velocity and induced magnetic field on MHD stagnation-point flow and heat transfer of Casson fluid over a stretching sheet,Hindawi Mathematical Problems in Engineering, 2018, 1-11. https://doi.org/10.1155/2018/9402836
12. Murtaza, M. G, Tzirtzilakis. E. E and Ferdows. M; Numerical solution of three-dimensional unsteady bio-magnetic flow and heat transfer through stretching/shrinking sheet using temperature dependent magnetization, Arch. Mech, 2018, 70 (2), 161–185.
13. Nandkeoyar.R, Narayana.M ,Motsa.S.S and Sibanda.P; Magnetohydrodynamic mixed convective flow due to a vertical plate with induced magnetic field , Journal of Thermal Science and Engineering Apllicatons,2018, doi:10,1115/1.4040644
14. Pai. S.I; Viscous flow theory I: Laminar flow, D. Van Nostrand Co, 1956, New York.
15. Raju.C.S.K, Sandeep.N and Saleem.S; Effects of induced magnetic field and homogeneous–heterogeneous reactions on stagnation flow of a Casson fluid, Engineering Science and Technology, an International Journal, 2016, 19,875–887.http://dx.doi.org/10.1016/j.jestch.2015.12.004
16. Raptis.A; Flow of a micropolar fluid past a continuously moving plate by the presence of radiation, Int. J. Heat Mass Transf.,1998, 41(18), 2865-2866.
17. Rossow.VJ; on flow of electrically conducting fluid over a flat plate in the presence of a transverse magnetic field. *NACA technical report* 3071, 1957.
18. Sandeep.N, Sulochana.C and AnimasaunI. L ; Stagnation-point flow of a Jeffrey nanofluid over a stretching surface with induced magnetic field and chemical reaction, International Journal of Engineering Research inAfrica,2016,20,93-111.doi.org/10.4028/www.scientific.net/JERA.20.93
19. Shateyi. S and Mabood. F;MHD mixed convection slip flow near a stagnation-point on a non-linearly vertical stretching sheet in the presence of viscous dissipation, Thermal Science, 2017, 21(6B), pp. 2709-2723.
20. Shit. G. C and Roy. M; Effect of induced magnetic field on blood flow through a constricted channel: an analytical approach, Journal of Mechanics in Medicine and Biology, 2016, 16(2), 1650030-49. DOI: 10.1142/S0219519416500305.
21. Stanford Shateyi and Gerald Tendayi Marewo; Numerical analysis of unsteady MHD flow near a stagnation point of a two-dimensional porous body with heat and mass transfer, thermal radiation and chemical reaction, 2014.http://www.boundary value problems.com/content/2014/1/218
22. Wang.C.Y; Stagnation flows with slip: exact solutions of the Navier-Stokes equations,ZAMP,2003, 54(1),184–189.